ISSN 0021-3640, JETP Letters, 2008, Vol. 88, No. 8, pp. 515–519. © Pleiades Publishing, Ltd., 2008.
Original Russian Text © V.G. Myagkov, L.E. Bykova, G.N. Bondarenko, V.S. Zhigalov, 2008, published in Pis'ma v Zhurnal Éksperimental'noĭ i Teoreticheskoĭ Fiziki, 2008, Vol. 88, No. 8, pp. 592–596.

Solid-Phase Synthesis of Solid Solutions in Cu/Ni(001) Epitaxial Nanofilms

V. G. Myagkov[a], L. E. Bykova[a], G. N. Bondarenko[b], and V. S. Zhigalov[a]

[a] *Kirensky Institute of Physics, Siberian Branch, Russian Academy of Sciences, Akademgorodok, Krasnoyarsk, 660036 Russia*

e-mail: miagkov@iph.krasn.ru

[b] *Institute of Chemistry and Chemical Technology, Siberian Branch, Russian Academy of Sciences, Krasnoyarsk, 660036 Russia*

Received August 20, 2008

Solid-phase synthesis of solid solutions in the epitaxial Cu/Ni(001) bilayer film systems of compositions 3Cu : 1Ni, 1Cu : 1Ni, and 1Cu : 3Ni has been studied using the X-ray diffraction methods. The saturation magnetization and the magnetic crystallographic anisotropy constant on nickel vary in accordance with the solid solution formation. The initiation temperature of the solid solutions is about 350°C and is independent of the Ni : Cu layer thickness ratio. The solid-phase synthesis of the solid solutions is presumably attributed to the transport of the Cu atoms to the epitaxial Ni(001) layer. It is found that the solid-phase synthesis in the Cu/Ni bilayer nanofilms and multilayers is determined by the spinodal decomposition in the Cu–Ni system.

PACS numbers: 66.30.Pa, 81.15.Np, 81.20.Ka, 81.30.Bx

DOI: 10.1134/S0021364008200101

INTRODUCTION

The Cu/Ni film systems have many unique properties including a strong perpendicular anisotropy (see [1] and references therein), an exchange interaction, a microwave giant magnetoresistance [2], and an anomalous spin-reorientation phase transition [3]. The magnetic measurements show that the Cu/Ni multilayers are not necessarily typical ferromagnets, but can be in the spin glass state, and the effect of the fusion of Cu and Ni at the interfaces is important for the formation of these properties [4]. The atomic mixing and formation of the layer compounds at the interface are critical for the breakdown of many effects in the thin film systems. For example, the diffusion of Ni into Cu leads to the irreversible degradation of giant magnetoresistance in the NiCo/Cu [5], NiFe/Cu [6, 7], NiFe/Cu/NiFe [8], and Co/Cu/NiFe [9] multilayers at high temperatures. It is assumed that the mixing at the interface of the Ni ultrathin layer and Cu causes a strong decrease in the magnetic moment of the Ni/Cu(001) films [10, 11]. Contradictory results are reported on the possible mixing at the Ni/Cu interface. On the one hand, the X-ray photoelectron diffraction [12] and the Auger electron spectroscopy [10] investigations of the Ni/Cu(001) films with increasing temperature indicate that surface fusion is possible in the temperature range 0–200°C. On the other hand, scanning electron microscopy studies do not imply any mixing at the Ni/Cu interface up to 450°C [13]. The stability conditions for the Ni/Cu film systems with an increase in temperature remain unclear primarily because general knowledge on the mechanisms of the chemical interaction at the nanolevel responsible for the mixing and formation of the compounds at the interface of the film reagents is absent.

In this work, we present the results of the solid-phase synthesis of the Cu_xNi_{1-x} solid solutions in the epitaxial Cu/Ni(001) nanofilms. The mixing at the Ni/Cu interface starts at about 350°C and is independent of the layer thickness ratio in the sample. Possible synthesis mechanisms are discussed. It is shown that the low-temperature synthesis of the solid solutions in the Cu/Ni(001) nanofilms is associated with the existence of spinodal decomposition in the Ni–Cu system.

SAMPLES AND EXPERIMENTAL PROCEDURE

The initial Cu/Ni(001) film structures were prepared by thermal evaporation onto the MgO(001) single-crystal substrate in a vacuum of 10^{-6} Torr. The samples used in the experiments on the layers bulk had the atomic ratio 3Cu : 1Ni, 1Cu : 1Ni, and 1Cu : 3Ni. The total thickness of the Cu/Ni(001) film structures did not exceed 250 nm. To obtain the epitaxial Ni(001) layer, nickel was deposited at about 250°C. Copper was deposited at room temperature and formed the polycrystalline layer. A strong diffraction reflection (002)Ni confirms the formation of the epitaxial Ni(001) layer, and weak reflections from Cu point to the formation of the polycrystalline Cu layer (see Fig. 2). These samples had the magnetic crystallographic anisotropy constant $K_1 = -6.0 \times 10^4$ erg/cm^3 (per Ni film volume) typical of the Ni single crystals. Easy axes of the Ni film coin-

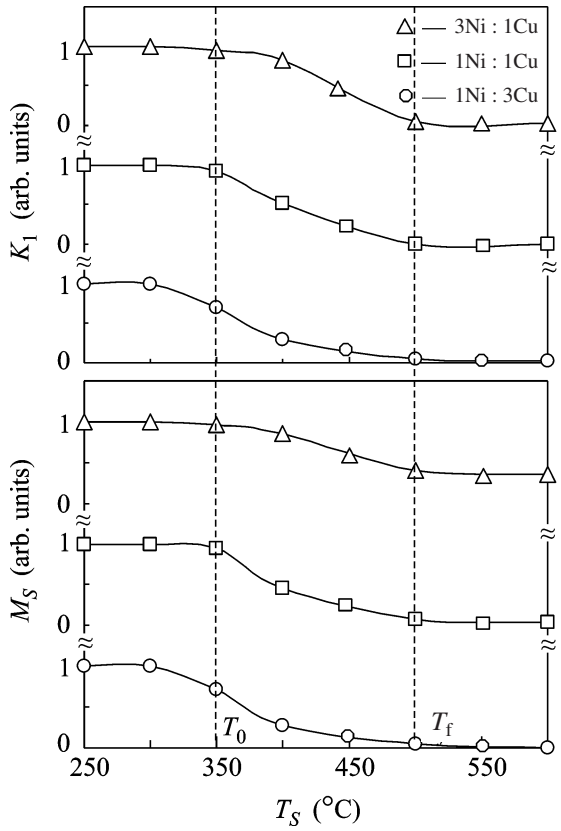

Fig. 1. (a) Normalized saturation magnetization M_S^{Ni} and (b) normalized magnetic crystallographic anisotropy constant K_1^{Ni} of nickel in the Cu/Ni(001) film samples of compositions 3Cu : 1Ni, 1Cu : 1Ni, and 1Cu : 3Ni versus the annealing temperature T_S. The vertical dashed lines mark the initiation, $T_0 \sim 350$°C, and termination, $T_f \sim 500$°C, temperatures of the solid-phase reaction.

cided with the [110] and [1–10] directions of the MgO(001) substrates. This indicates the existence of the orientation ratios [100], (001)Ni || [100],(001)MgO in the epitaxial growth of nickel on the MgO(001) surface. These two factors show the crystal perfection of the initial Ni(001) layers prepared under the given technological conditions. The Ni(001) films grow epitaxially in a similar way on the MgO(001) surface in an ultrahigh vacuum [14].

The prepared samples were successively annealed from 250 to 800°C with a step of 50°C for 30 min at each temperature. The phases thus formed were identified using the X-ray diffraction studies on a DRON-4-07 diffractometer (CuK_α radiation). The X-ray fluorescence spectral method was used to determine the chemical composition and thickness of the films. The magnetic crystallographic anisotropy K_1 and the saturation magnetization M_S were measured using the torque method with a maximum magnetic filed of 18 kOe

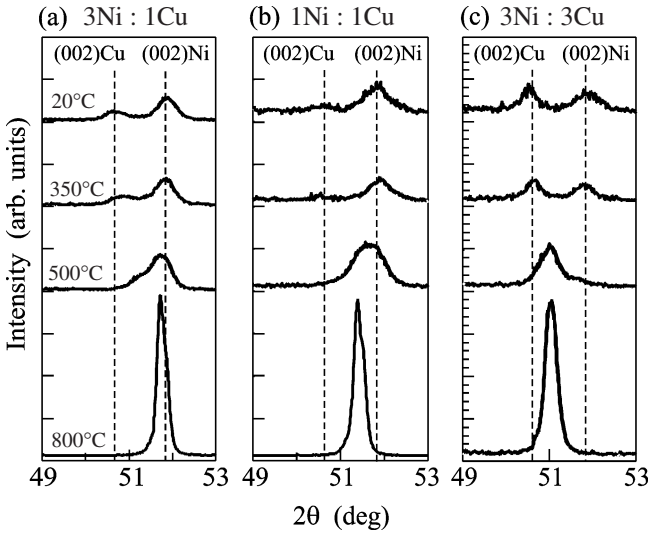

Fig. 2. Diffraction patterns of the epitaxial Cu/Ni(001) film system of compositions 3Cu : 1Ni, 1Cu : 1Ni, and 1Cu : 3Ni at different annealing temperatures.

according to the technique described in [15]. The measurements were performed at room temperature.

EXPERIMENTAL RESULTS

Figure 1 presents the normalized magnetic crystallographic anisotropy constant $K_1^{Ni}(T_S)$ and normalized saturation magnetization $M_S^{Ni}(T_S)$ as functions of the annealing temperature T_S. Up to 300°C, K_1^{Ni} and M_S^{Ni} are independent of the temperature T_S in all of the samples. This proves the absence of the mixing and formation of the compounds at the Ni/Cu interface. At a temperature near 350°C, K_1^{Ni} and M_S^{Ni} decrease in the single-crystalline Ni(001) layer of all samples. Nickel shows no structural transformations up to 800°C. Therefore, any decrease in the magnetic crystallographic anisotropy constant $K_1^{Ni}(T_S)$ of nickel and the saturation magnetization $M_S^{Ni}(T_S)$ of the Cu/Ni(001) bilayer film with annealing temperature T_S is attributed to the solid-phase synthesis between the Ni and Cu layers. Therefore, the temperature $T_0 \sim 350$°C is the synthesis initiation temperature. At temperatures above $T_f \sim 500$°C, K_1^{Ni} and M_S^{Ni} are zero for the samples with the atomic ratios (a) 3Cu : 1Ni and (b) 1Cu : 1Ni and are constant for the films with the (c) 1Cu : 3Ni atomic ratio. This suggests that the Ni and Cu layers are fully mixed at this temperature and synthesis is completed.

Figure 2 shows the evolution of the (002)Ni and (002) Cu peaks in the Cu/Ni(001) bilayer films for the (a) 3Cu : 1Ni, (b) 1Cu : 1Ni, and (c) 1Cu : 3Ni compositions in the annealing up to 800°C. The diffraction

patterns at the synthesis initiation temperature T_0 ~ 350°C for all three compositions only slightly differ from those for the initial samples and show the formation of a reflection between the (002)Ni and (002)Cu peaks. At the synthesis finish temperature T_f ~ 500°C, the diffraction patterns change radically. The (002)Ni and (002)Cu peaks disappear and new strong intermediate composition-dependent reflections appear (Fig. 2). As the annealing temperature increases up to 800°C, these reflections increase strongly, indicating the structural perfection of the synthesis products. The formation of the intermediate reflection between the (002)Cu and (002)Ni peaks shows that the products of the solid-phase reaction between Ni and Cu are the fcc solid solutions Cu_xNi_{1-x}, where the concentration is determined by the atomic ratio of the layers of the initial Cu/Ni(001) film structures. This implies that the reacted Cu/Ni(001) samples of the compositions 3Cu : 1Ni, 1Cu : 1Ni, and 1Cu : 3Ni contain the $Cu_{75}Ni_{25}$, $Cu_{50}Ni_{50}$, and $Cu_{25}Ni_{75}$ solid solutions, respectively, and the diffraction patterns have the (002)$Cu_{75}Ni_{25}$, (002)$Cu_{50}Ni_{50}$, and (002)$Cu_{25}Ni_{75}$ peaks (see Fig. 2). The presence of only the strong (002)$Cu_{75}Ni_{25}$, (002)$Cu_{50}Ni_{50}$, and (002)$Cu_{25}Ni_{75}$ reflections implies the directional growth of these films on the (001)MgO surface: (001)$Cu_{75}Ni_{25}$ || (001)MgO, (001)$Cu_{50}Ni_{50}$ || (001)MgO, and (001)$Cu_{25}Ni_{75}$ || (001)MgO. Further annealings up to 800°C do not produce new phases. This means that the phase sequence Cu/Ni $\longrightarrow$ (~350°C)Cu_xNi_{1-x} forms in the Cu/Ni film system. The above consideration allows the following scenario of the solid-phase synthesis of the solid solutions in the epitaxial Cu/Ni(001) bilayer films. Up to T_0 ~ 350°C, the Cu/Ni interface remains sharp. However, above the synthesis initiation temperature T_0, the Cu/Ni(001) film system transfers to the excited state; as a result, the Cu atoms migrate to the epitaxial Ni(001) layer, are involved in the solid-phase reaction with Ni, and form the solid solution. This scenario presumes the solid-phase epitaxial growth of the solid solution on the MgO(001) surface with the orientation relations [100],(001)Cu_xNi_{1-x} || [100],(001)MgO. The lattice parameters of the Cu_xNi_{1-x} alloys determined from the (002)$Cu_{75}Ni_{25}$, (002)$Cu_{50}Ni_{50}$, and (002)$Cu_{25}Ni_{75}$ reflections decrease as the Ni content increases (Fig. 3) and satisfy Vegard's rule within the experimental error. The magnetic measurements show that only the $Cu_{25}Ni_{75}$ alloy samples remain ferromagnetic after the reaction, and these films have the first magnetic crystallographic anisotropy constant close to zero at room temperature (see Fig. 1).

DISCUSSION OF THE RESULTS

The unique property of solid-phase synthesis in thin films is that only one phase (*the first phase*) is formed at the interface as the temperature increases to T_0 (*the initiation temperature*), although several phases may exist according to the phase diagram. As the annealing temperature is further increased, other phases can also be formed in *the phase sequence*. Various models explaining the initiation of the first phase and the formation of the phase sequence are proposed in [16, 17] and the references therein. However, no general model can predict the *first phase, phase sequence, and their initiation temperature* for the entire variety of binary systems.

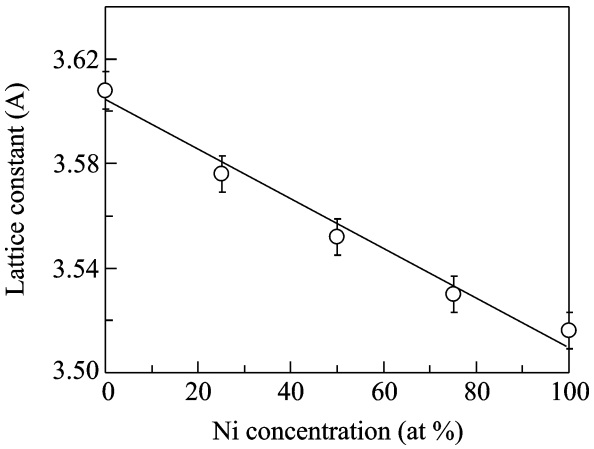

Fig. 3. Lattice constant of the Cu_xNi_{1-x} solid solution versus the Ni concentration.

The thin bilayer metal films and multilayers can be considered as alloys with the one-dimensional nanostructure formed artificially along the normal. Therefore, as the temperature increases, the processes of mixing and phase formation in such systems, as well as in the alloys, should follow the diagram of phase equilibrium. It was shown in [18–25] that, at the interface of the film reagents,

(i) *the first phase appears at the minimum temperature T_K of an arbitrary structural solid-phase transformation in a given binary system*;

(ii) *the initiation temperature T_0 of the first phase coincides with T_K ($T_0 = T_K$).*

This assumption is valid for many structural transformations. In particular, the mixing in the Al/Ge thin films begins at the eutectic temperature in the Al–Ge system [18]. The solid-phase reactions in S/Fe [19], Cu/Au [20], and Se/Cu [21] begin at the temperatures of the standard phase transitions (the metal–insulator, order–disorder, and the superionic transitions), which have the lowest temperature among the structural phase transformations in the Fe–S, Cu–Au, and Se–Cu systems, respectively. The martensitic transformations are the diffusion-free transformations. However, the low-temperature solid-phase reactions in the Ni/Ti, Au/Cd, and Al/Ni bilayer films start at temperatures A_S of the inverse martensitic transformation in the NiTi [22, 23], AuCd [22, 24], and AlNi [22, 25] phases.

The suggested first-phase rule provides a one-to-one relation between its initiation temperature T_0 and the temperature T_K of the structural transformation having the minimum temperature in a given binary system. Therefore, if the low-temperature part of the constitution diagram is well established, it can then be used to predict the reaction initiation temperature and the first phase in the corresponding bilayer nanofilms and multilayers. At the same time, the study of the solid-phase reactions in the bilayer nanofilms makes it possible to refine the diagram of constitution of the given binary system.

The high-temperature part of the Cu–Ni phase equilibrium diagram has been well determined, and it has been experimentally shown that copper and nickel have unlimited solubility in the solid state and form a continuous series of solid solutions based on the fcc lattice from pure nickel to pure copper [26]. At low temperatures, the homogeneous solid solution undergoes spinodal decomposition. The thermodynamic calculations predict the discontinuity in miscibility at a temperature below $T_{SPIN} = 600$ K [26–28]. Owing to low diffusion mobility at these temperatures, it is very difficult to obtain direct experimental evidence of the decomposition and to accurately measure the spinodal temperature. With the use of neutron irradiation in order to increase the atomic mobility, the coherent spinodal temperature $T_{SPIN} = 525$ K was determined for the Ni–41 at % Cu compound [28]. The Ni–30 at % Cu alloy has a value close to the coherent spinodal temperature $T_{SPIN} = 590$ K [29].

The Cu–Ni phase diagram exhibits only the spinodal decomposition and does not include any other solid-phase transformations. According to the above first-phase rule, the atomic mixing at the Cu/Ni interface should begin at the coherent spinodal temperature ($T_0 = T_{SPIN}$), and the reacted samples should contain the fcc Cu_xNi_{1-x} solid solutions. In other words, the fcc Cu_xNi_{1-x} solid solution is the first (and only) phase formed at the Cu/Ni interface at the spinodal decomposition temperature. Actually, the close experimental values of T_0 and T_{SPIN} imply the existence of the equality $T_0 = T_{SPIN}$. This result and the formation of the solid solutions in the reacted samples clearly demonstrate that the phase formation in the Cu/Ni film structures follows the above first-phase rule. Since the initiation temperature T_0 is the same for the 3Cu : 1Ni, 1Cu : 1Ni, and 1Cu : 3Ni samples, the coherent spinodal temperature T_{SPIN} is independent of the composition. Thus, we assume that the Ni–Cu phase diagram contains the coherent spinodal whose temperature for the compounds with the Ni concentration ranging from 25 to 75 at % is independent of the composition ($T_{SPIN} \sim$ 350°C). This conclusion is inconsistent with the thermodynamic calculation results presented on the modern phase equilibrium diagram where the solubility boundary has the maximum temperature 354.5°C at the Cu–67 at % Ni composition [26].

The threshold character is important for the solid-phase synthesis in the nanofilms. In particular, the atomic exchange is absent in the Cu/Ni samples up to 300°C. Since the diffusion coefficient is low, $D < 10^{-20}$ cm^2/s, up to 350°C [30], any atomic transport through the Cu/Ni interface is absent for a characteristic annealing time of 30 min, $d \sim (Dt)^{1/2} = 10^{-8}$ cm ~ 0. However, the diffusion coefficient increases sharply by six or seven orders of magnitude as the temperature becomes higher than the initiation temperature $T_0 \sim 350$°C, $D = d^2/t \sim 10^{-13}$ cm^2/s. This result contradicts the Arrhenius temperature dependence of the diffusion coefficient. This means that the chemical interaction between the Cu and Ni atoms, which was absent up to the initiation temperature $T_0 \sim 350$°C, increases sharply in the transition through T_0. The chemical interaction induces the directed fast transport of the Cu atoms into the Ni(001) layer and the epitaxial growth of the solid solutions.

CONCLUSIONS

We have studied the phase formation in the epitaxial Cu/Ni(001) nanofilms of compositions 3Cu : 1Ni, 1Cu : 1Ni, and 1Cu : 3Ni as the annealing temperature increases up to 800°C. In all the samples, the atomic mixing and formation of the solid solution start at the initiation temperature $T_0 \sim 350$°C and is completed at $T_f \sim 500$°C. The formation of the epitaxial solid solution implies that the solid-phase synthesis mechanism involves the migration of the Cu atoms into the Ni(001) layer without any change in the orientation relations with the MgO(001) substrate. Analysis of the solid-phase reactions in the nanofilms allows us to attribute the solid-phase synthesis of the solid solution at the Cu/Ni interface to the spinodal decomposition in the Cu–Ni system. In this case, the coherent spinodal temperature coincides with the initiation temperature, $T_{SPIN} = T_0 \sim 350$°C.

This work was supported by Russian Foundation for Basic Research (project no. 07-03-00190).

REFERENCES

1. C. A. Vaz, J. A. C. Bland, and G. Lauhoff, Rep. Prog. Phys. **71**, 056501 (2008).
2. B. K. Kuanr, S. Gokhale, M. Vedpathak, et al., J. Phys. D: Appl. Phys. **33**, 34 (2000).
3. M. Farle, W. Platow, A. N. Anisimov, et al., Phys. Rev. B **56**, 5100 (1997).
4. W. Abdul-Razzaq, J. Appl. Phys. **67**, 4907 (1990).
5. Y. An1, J. Liu, Y. Ma, and R. Ji, J. Phys. D: Appl. Phys. **41**, 035001 (2008).
6. M. Hecker, D. Tietjen, and C. M. Schneider, Appl. Phys. Lett. **91**, 7203 (2002).
7. C. B. Ene, G. Schmitz, R. Kirchheim, et al., Surf. Interface Anal. **39**, 227 (2007).

8. W. Bruckner, S. Baunack, M. Hecker, et al., Appl. Phys. Lett. **77**, 358 (2000).
9. J. Schleiwies, G. Schmitz, S. Heitmann, et al., Appl. Phys. Lett. **78**, 3439 (2001).
10. P. Srivastava, F. Wilhelm, A. Ney, et al., Phys. Rev. B **58**, 5701 (1998).
11. A. Meunier, B. Gilles, and M. Verdier, Appl. Surf. Sci. **212–213**, 171 (2003).
12. B. Hernnas, M. Karolewski, H. Tillborg, et al., Surf. Sci. **302**, 64 (1994).
13. J. Shen, J. Giergiel, and J. Kirschner, Phys. Rev. B **52**, 8454 (1995).
14. Z. Zhang, R. A. Lukaszew, C. Cionca, et al., J. Vac. Sci. Technol. A **22**, 1868 (2004).
15. S. Chikazumi, J. Appl. Phys. **32**, S81 (1961).
16. R. Pretorius, C. C. Theron, A. Vantomme, et al., Crit. Rev. Solid. State Mater. Sci. **24**, 1 (1999).
17. T. Laurila and J. Molarius, Crit. Rev. Solid. State Mater. Sci. **28**, 185 (2003).
18. V. G. Myagkov, L. E. Bykova, and G. N. Bondarenko, Zh. Éksp. Teor. Fiz. **115**, 1756 (1999) [JETP **88**, 963 (1999)].
19. V. G. Myagkov, L. E. Bykova, V. S. Zhigalov, et al., Dokl. Akad. Nauk **371**, 763 (2000) [Phys. Dokl. **45**, 157 (2000)].
20. V. G. Myagkov, L. E. Bykova, V. S. Zhigalov, et al., Pis'ma Zh. Éksp. Teor. Fiz. **71**, 268 (2000) [JETP Lett. **71**, 183 (2000)].
21. V. G. Myagkov, L. E. Bykova, and G. N. Bondarenko, Dokl. Akad. Nauk **390**, 35 (2003) [Phys. Dokl. **48**, 206 (2003)].
22. L. E. Bykova, V. G. Myagkov, and G. N. Bondarenko, Khimiya Inter. Ustoich. Razvit. **13**, 137 (2005).
23. V. G. Myagkov, L. E. Bykova, L. A. Li, et al., Dokl. Akad. Nauk **382**, 463 (2002) [Phys. Dokl. **47**, 95 (2002)].
24. V. G. Myagkov, L. E. Bykova, and G. N. Bondarenko, Dokl. Akad. Nauk **388**, 46 (2003) [Phys. Dokl. **48**, 30 (2003)].
25. V. G. Myagkov, L. E. Bykova, S. M. Zharkov, and G. N. Bondarenko, Solid State Phenom. **138**, 377 (2008).
26. T. B. Massalski, *Binary Alloy Phase Diagrams*, 2nd Ed. (ASM, Metals Park, OH, 1990).
27. D. G. Kim and W. K. Choo, Scripta Metall. **19**, 1415 (1985).
28. S. Mey, Z. Metallkd. **78**, 502 (1987).
29. V. M. Lopez Hirata and K.-I. Hirano, J. Mater. Sci. **31**, 1703 (1996).
30. T. Tsakalakos, Thin Solid Films **86**, 79 (1981).

Translated by E. Perova